
USING SYNTHETIC CORRUPTIONS TO MEASURE ROBUSTNESS TO NATURAL DISTRIBUTION SHIFTS

A PREPRINT

Alfred LAUGROS
alfred.laugros@atos.net
Atos, France

Alice CAPLIER
alice.caplier@grenoble-inp.fr
Universite Grenoble Alpes, France

Matthieu OSPICI
matthieu.ospici@atos.net
Atos, France

ABSTRACT

Synthetic corruptions gathered into a benchmark are frequently used to measure neural network robustness to distribution shifts. However, robustness to synthetic corruption benchmarks is not always predictive of robustness to distribution shifts encountered in real-world applications. In this paper, we propose a methodology to build synthetic corruption benchmarks that make robustness estimations more correlated with robustness to real-world distribution shifts. Using the overlapping criterion, we split synthetic corruptions into categories that help to better understand neural network robustness. Based on these categories, we identify three parameters that are relevant to take into account when constructing a corruption benchmark: number of represented categories, balance among categories and size of benchmarks. Applying the proposed methodology, we build a new benchmark called ImageNet-Syn2Nat to predict image classifier robustness.

1 Introduction

Neural networks have been shown to be sensitive to distribution shifts such as common corruptions [Hendrycks and Dietterich, 2019], adversarial examples [Szegedy et al., 2014] or background changes [Beery et al., 2018]. When deployed in real-world environments, neural networks often encounter samples that come from a different distribution than the one used to train them. Because of this, they obtain lower performances in practical applications compared to the performances observed on their test sets. In most cases, during model conceptions, we do not have access to the distributions that these models will encounter when deployed in real world applications. Consequently, it is necessary to make neural networks more robust to distribution shifts.

Some methods have been proposed to make neural networks more robust to distribution shifts [Rusak et al., 2020, Xie et al., 2020a,b]. To estimate if these methods are useful in practice, we need to establish benchmarks that measure robustness to distribution shifts. Traditionally used approaches consist in measuring performances of models on out-of-distribution samples, i.e. samples that come from a different distribution than the one used to get the training samples. The underlying idea is that the more a model has good performances on an unseen distribution, the more we can expect it to be robust to other unseen distribution shifts.

However, there is no guarantee that the robustness measured using one particular distribution transfers to other distributions: a model robust to colorimetry variations is not necessarily robust to background changes. To address this issue, we generally use several distributions during the testing phase, to have more diverse out-of-distribution samples. We assume that the more a model is robust to a large diversity of distribution shifts, the more this model is likely to generalize to other unseen distributions. For this reason, finding new distributions to draw more diverse test samples, can be useful to improve robustness estimations.

Various distribution shifts can be obtained by using synthetic corruptions such as Gaussian noise, rotations, contrast loss... The robustness of a model can be estimated by testing its performances on a test set that has been corrupted using various image transformations. In this paper, we make a distinction between synthetic and natural corruptions. Synthetic corruptions correspond to modeled images transformations that are used to corrupt images such as translations or quantizations. On the other hand, natural corruptions are distribution shifts arising naturally in real world applications

[Taori et al., 2020]. In this study, we do not consider transformations especially crafted to fool neural networks such as adversarial attacks [Szegedy et al., 2014].

Constituting a benchmark of naturally corrupted samples is costly. It requires to draw samples from a distribution that is not covered by existing datasets, and to label the gathered samples. Samples corrupted with synthetic corruptions are cheaper to gather. They can be obtained by corrupting already labeled images. However, we do not really know in which circumstances robustness to synthetic corruptions is predictive of robustness to natural corruptions [Taori et al., 2020, Hendrycks et al., 2020]. Besides, it has been shown that synthetic corruption benchmarks can be biased, i.e. they give too much importance to the robustness to some kinds of corruptions and omit some others [Laugros et al., 2021].

To address these limitations, we propose a new methodology to build synthetic corruption benchmarks. More precisely, given an initial set of synthetic corruptions, we split this set into specific categories. These categories are built such as the corruptions belonging to the same category overlap (they are correlated in terms of robustness), while the corruptions belonging to different categories do not. Based on these corruption categories, we identify three parameters to take into account while building a synthetic corruption benchmark: (1) the number of represented corruption categories (2) the balance among categories (3) the size of benchmarks. We show that considering these parameters helps to build synthetic corruption benchmarks that make robustness estimations more correlated with robustness to natural corruptions. We apply the proposed methodology to build a new benchmark called ImageNet-Syn2Nat that is used to measure the robustness of ImageNet classifiers.

2 Background

Robustness Estimations. Several benchmarks have been proposed to estimate robustness of image classifiers to naturally occurring corruptions. For instance, SVSF is a store front classification dataset that reveals the natural corruptions that arise when varying three parameters: camera, year and country [Hendrycks et al., 2020]. The SI-Score dataset focuses on the robustness to other parameters such as object size, location and orientation [Djolonga et al., 2021]. Robustness to background changes is also a widely studied topic [Beery et al., 2018]. A lot of robustness benchmarks have been proposed to measure robustness of ImageNet classifiers. ImageNet-A is a challenging benchmark, constructed by selecting images that are misclassified by various ResNet 50 architecture based models [Hendrycks et al., 2021]. ImageNet-V2 [Recht et al., 2019] has been built by replicating the ImageNet construction process. Because of some statistical biases in the image selection [Engstrom et al., 2020], a distribution shift is observed between ImageNet and ImageNet-V2. ObjectNet [Barbu et al., 2019] is a set of images that contains objects that have been randomly rotated or taken with various backgrounds and viewpoints. ImageNet-R contains artistic renditions of ImageNet object classes [Hendrycks et al., 2020]. ImageNet-Vid [Shankar et al., 2019] and ImageNet-P [Hendrycks and Dietterich, 2019] study stability of model predictions on sequences of similar images. ImageNet-D has been recently proposed to provide additional challenging distribution shifts (quickdraw, infograph...) [Rusak et al., 2021].

ImageNet-C is a synthetic corruption benchmark widely used to estimate robustness of ImageNet classifiers [Hendrycks and Dietterich, 2019]. It contains fifteen corruptions which can be classified into noises, blurs, weather and digital corruptions. Other synthetic corruption benchmarks have been proposed to evaluate robustness of neural networks in various computer vision tasks such as face recognition [Karahan et al., 2016], object detection [Michaelis et al., 2019], image segmentation [Kamann and Rother, 2020], saliency region detection [Che et al., 2020], traffic sign recognition [Temel et al., 2017] and scene classification [Tadros et al., 2019].

Corruption Overlappings. Two synthetic corruptions overlap when they are correlated in terms of robustness. For instance, it has been demonstrated that corruptions that damage high frequencies in images (noises, blurs...) overlap [Yin et al., 2019, Laugros et al., 2019]. It has been shown that a benchmark should not contain a couple of corruptions c_1, c_2 such as c_1 overlaps much more with the other corruptions of the benchmark than c_2 [Laugros et al., 2021]. Otherwise, the considered benchmark gives too much importance to the robustness towards some kinds of corruptions compared to others. The overlapping score metric [Laugros et al., 2021] has been recently proposed to measure to what extent two corruptions c_1 and c_2 overlap:

$$O_{c_1, c_2} = \max\left\{0, \frac{1}{2} * \left(\frac{R_{c_2}^{m_1} - R_{c_2}^{standard}}{R_{c_2}^{m_2} - R_{c_2}^{standard}} + \frac{R_{c_1}^{m_2} - R_{c_1}^{standard}}{R_{c_1}^{m_1} - R_{c_1}^{standard}} \right)\right\} \quad (1)$$

m_1, m_2 and *standard* are models with the same architecture. m_1 and m_2 have been respectively trained with data augmentation on c_1 and c_2 ; *standard* is only trained on clean samples. R_c^m is the ratio between the accuracy of m on samples corrupted with c and the accuracy of m on not-corrupted samples. The idea behind the overlapping score is that the more a data augmentation with c_1 makes a model robust to c_2 and conversely, and the more we can suppose that c_1 and c_2 are correlated in terms of robustness. The overlapping range value is [0-1]. The higher this score is, the more the considered corruptions overlap.

Architecture	Robustness Intervention
ResNet18	FastAutoAugment [Lim et al., 2019]; Worst-of-10 spatial data augmentation using the following transformation space: ± 3 pixels ± 30 degrees [Engstrom et al., 2019]
ResNet-50	ANT ^{3x3} [Rusak et al., 2020]; SIN Augmentation [Geirhos et al., 2019]; Augmix [Hendrycks* et al., 2020]; DeepAugment [Hendrycks et al., 2020]; MoPro [Li et al., 2021]; RSC [Huang et al., 2020]; Adversarial Training: $L_{inf}, \epsilon = 4/256$ [Madry et al., 2018]
EfficientNet-0	Noisy Student Training [Xie et al., 2020b]; AdvProp [Xie et al., 2020a]
DenseNet-121	Anti-Aliased [Vasconcelos et al., 2020]
ResNet-152	Cutmix [Yun et al., 2019]
ResNeXt-101-32x16d	Weakly Supervised Pretraining [Mahajan et al., 2018]; Semi-Supervised Pretraining [Yalniz et al., 2019]

Table 1: Selection of fifteen models, each trained using a different robustness intervention.



Figure 1: Candidate corruptions displayed in the same order as the corruption names of Figure 2.

Experimental Set-up. All overlapping scores computed in this paper, are obtained using the ImageNet-100 dataset (a subset of ImageNet that contains every tenth ImageNet class by WordNetID order [Deng et al., 2009]), the ResNet-18 architecture, and exactly the same training hyperparameters as the ones used in the paper introducing the overlapping score [Laugros et al., 2021].

In all experiments, we measure the robustness of an image classifier f to a distribution P by computing the residual robustness: $R(f, P) = A_{i.i.d.}(f) - A_P(f)$. $A_{i.i.d.}(f)$ and $A_P(f)$ are the accuracies of f respectively computed with *i.i.d.* samples (independent and identically distributed samples with regard to the training set of f) and samples drawn from P . Other robustness metrics could have been used [Taori et al., 2020, Hendrycks and Dietterich, 2019], but we choose the residual robustness because it is how robustness is generally considered in industrial applications: it is the accuracy drop caused by a distribution shift. We note that comparing the residual robustness of two models to a distribution shift, requires to check that the accuracies on *i.i.d.* samples of the two models are comparable. This condition is verified in all our experiments. In this paper, the robustness of a model f to a synthetic corruption benchmark *bench*, refers to the mean of the residual robustnesses of f computed with the corruptions of *bench*.

Some experiments in this paper require to select models that have been shown to be robust to some out-of-distribution shifts. The used selection is displayed in Table 1.

3 Corruption Categories

There are a lot of possible synthetic corruptions that can be included in a benchmark. Constructing a corruption benchmark requires to pick some corruptions among all possible candidates. Here, we consider a list of 40 candidate corruptions whose names can be seen in the abscissa of Figure 2 and that are illustrated in Figure 1. An other list of corruptions could have been selected, but most of the corruptions that are usually included in existing benchmarks [Temel et al., 2017, Karahan et al., 2016, Hendrycks and Dietterich, 2019] can be found in these candidates: blurs, noises, contrast loss... The 40 corruptions are implemented thanks to the alumentations library [Buslaev et al., 2020], the function parameters used to model these corruptions can be found at [Link available upon acceptance].

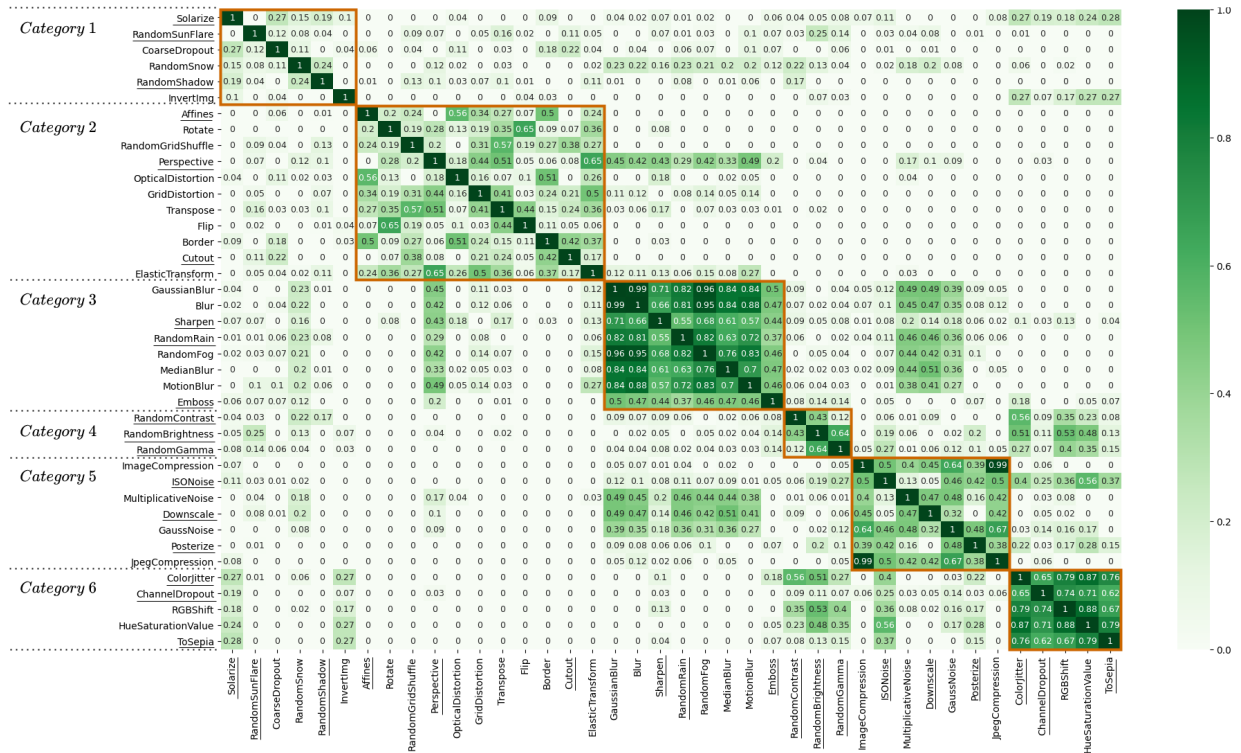


Figure 2: Overlapping scores computed using all the possible candidate corruption couples. The scores computed with SCC are in the 6 orange squares: one square for each of the 6 categories.

The 40 considered corruptions form a heterogeneous set. It is difficult to determine the number and the kinds of corruptions to be included in a robustness benchmark a priori. In this paper, we propose a method to select groups of corruptions that make robustness estimations more correlated with robustness to natural corruptions.

The first step of our method is to compute the overlapping relations between candidate corruptions: here we use the correlations displayed in Figure 1. Each corruption c is then associated with a vector that contains all the overlapping scores computed using c and any other corruptions. The second step is to split the candidate corruptions into categories, such as the overlapping score vectors of the corruptions belonging to the same category are correlated; while the overlapping score vectors of the corruptions belonging to different categories are not. To achieve it, we cluster our candidates using their associated 40-dimensional vector of overlapping scores. We use the K-means algorithm increasing progressively the number of centroids K . We note that increasing K , raises on average the correlations between the overlapping vectors of the Same Category Corruptions (SCC), which is consistent with our goal; but it also raises the correlations between the vectors of Different Category Corruptions (DCC), which is not desired. We choose to stop increasing K at $K = 6$, when the mean of all the Pearson correlation coefficients computed using SCC overlapping vectors becomes higher than 0.5. The obtained categories can be seen in Figure 2.

We observe that all these categories do not contain the same number of corruptions. We also notice that SCC can be associated with a human visual perception interpretation for most of the categories. Indeed, *Category 2* to *6* in Figure 2, could be respectively called *spatial transformations*, *blurs*, *lightning condition variations*, *fine-grain artifacts* and *color distortions*. Note that the SCC of *Category 1* overlap way less than the ones of other categories because it contains more heterogeneous corruptions. Corruptions of *Category 1* would likely have been distributed between more refined categories by using additional corruptions in our initial set of candidates.

Empirical Evaluation. We conduct an additional experiment to verify the relevance of the built corruption categories. For each corruption c among the candidate corruptions displayed in Figure 1, we compute the residual robustness of the fifteen robust models displayed in Table 1 with the ImageNet validation set corrupted with c . Each candidate corruption c is now associated with a vector that contains the fifteen robustness scores computed using c . For each possible couple of candidate corruptions, we compute the Pearson correlation coefficient using the two robustness scores vectors associated with the corruptions of the considered couple. The mean correlation obtained using SCC

is 0.68, while the one obtained using DCC is 0.10. This experiment confirms the relevance of the built corruption categories: SCC are in practice correlated in terms of robustness while DCC are not.

4 Synthetic Corruption Selection Criteria

We introduce the definition of some terms used in this paper. The size of a benchmark is the number of corruptions this benchmark contains. Each time a benchmark *bench*, contains a corruption *c* that belongs to the corruption category *CC*, we say that *CC* is represented in *bench*; and *c* is called a representative of *CC* in *bench*. In this section, we identify three parameters of synthetic corruption benchmarks that influence the way robustness to these benchmarks is correlated with robustness to natural corruptions. These parameters are: (1) the number of corruption categories represented (2) the balance among categories (3) the size of benchmarks. We make an ablation study in each of the three following sections to demonstrate the importance of each parameter.

4.1 Number of Corruption Categories Represented in Benchmarks

Each corruption category displayed in Figure 2 contains image transformations that modify different attributes in images. For instance, *Category 6* contains essentially corruptions that modify colorimetry; while *Category 4* contains corruptions that modify contrast and brightness. As a consequence, the features modified in one category, are mostly different from the ones modified in the other categories. Then, we make the assumption that the more corruption categories are represented in a benchmark, the more this benchmark takes into account a large diversity of attribute modifications. Distribution shifts due to natural corruptions generally change a lot of attributes at the same time: background, resolution, viewpoint... Then, intuitively, the largest the number of represented categories in a benchmark is, the more this benchmark is likely to make robustness estimations predictive of robustness to natural corruptions. To verify this intuition, we propose to use Algorithm 1 to build several benchmarks that have various numbers of represented categories.

Algorithm 1 Corruption Benchmark Generation Algorithm

Require: A group of candidate corruptions split into several corruption categories *cat*

Require: *n*: the number of categories represented in the returned benchmark

Require: *k*: the number of representatives of the categories represented in the returned benchmark

Randomly select *n* categories in *cat*

For each selected category, randomly select *k* distinct corruptions of this category

return A benchmark that contains the selected corruptions

Using the corruption categories displayed in Figure 2, we run Algorithm 1 for several *n, k* couples: (2,3),(3,2),(6,1),(4,3),(6,2). We repeat this process until we obtain a group of 1000 different benchmarks for each of the considered *n, k* couples. We note that a benchmark generated using *n = 4, k = 3* contains 3 representatives of 4 out of 6 categories. We want to measure if increasing the number of represented categories *n* make robustness estimations of benchmarks more correlated with robustness to natural corruptions. To verify this, we propose the Algorithm 2, that measures to what extent the robustness estimations made by a group of synthetic corruption benchmarks, are on average correlated with the robustness to one natural corruption benchmark. For each of the benchmark groups generated using Algorithm 1, we run Algorithm 2 for each of the following natural corruption benchmarks: ImageNet-A [Hendrycks et al., 2021], ImageNet-R [Hendrycks et al., 2020], ImageNet-V2 [Recht et al., 2019] and ObjectNet [Barbu et al., 2019]. The group of neural networks used to run Algorithm 2 is the set of robust models presented in Table 1. The obtained results are displayed in Table 2.

Algorithm 2 Estimates the average correlation between the robustness to one natural corruption benchmark and the robustnesses to synthetic corruption benchmarks

Require: *SB* a group of synthetic corruption benchmarks

Require: *TNN* a group of trained neural networks

Require: *NB* a benchmark of naturally corrupted samples

scores₁ ← the residual robustness of all models in *TNN* computed with *NB*

For each benchmark *sb* in *SB*:

scores₂ ← the residual robustness of all models in *TNN* computed with *sb*

Get the Pearson correlation coefficient between *score₁* and *score₂*

return the mean of the correlation coefficients computed in the loop

	$n; k : 2; 3$	$n; k : 3; 2$	$n; k : 6; 1$	$n; k : 4; 3$	$n; k : 6; 2$	$n; k : 6; 3$
ImageNet-A	0.685	0.696	0.735	0.739	0.764	0.769
ImageNet-R	0.635	0.654	0.692	0.693	0.717	0.725
ImageNet-V2	0.696	0.742	0.785	0.789	0.806	0.814
ObjectNet	0.692	0.722	0.764	0.768	0.787	0.798

Table 2: Correlation scores computed using Algorithm 2 between natural corruption benchmarks and groups of synthetic corruption benchmarks built using Algorithm 1 for various n, k couples.

The higher an obtained score is, the more the synthetic corruption benchmarks of a considered group, make on average robustness estimations correlated with the robustness to the natural corruption benchmark used to compute the score. To only study the effect of the number of represented categories n in benchmarks, we only compare the scores of Table 2 obtained using benchmarks that have the same size. So, we compare the benchmarks of 6 corruptions generated using the (n, k) couples $(2, 3)$, $(3, 2)$ and $(6, 1)$. We see that the obtained scores increase with n for all the tested natural corruption benchmarks. Similarly, for the benchmarks of 12 corruptions generated using the (n, k) couples $(4, 3)$ and $(6, 2)$, the obtained scores are higher for $n = 6$ than $n = 4$. This experiment confirms the idea that increasing the number of categories represented in synthetic corruption benchmarks, makes robustness to these benchmarks more predictive of robustness to natural corruptions.

4.2 Balance Among Categories

We consider that the balance among categories represented in a benchmark is preserved, when all represented categories of this benchmark have the same number of representatives. For instance, the balance among categories of a benchmark *bench* that contains the Gaussian noise, iso-noise, multiplicative noise and color-jitter corruptions is not preserved: *bench* contains three representatives of *Category 5* and one representative of *Category 6* (see Figure 2). Obviously *bench* is biased towards texture damaging robustness rather than colorimetry variation robustness. Intuitively, the robustness to a benchmark biased towards a few kinds of feature modifications, is not likely to be predictive of robustness to natural corruptions that change a large diversity of features in images. Consequently, preserving the balance among categories, should help to build benchmarks that make robustness estimations more correlated with robustness to natural corruptions.

We conduct an experiment to verify this intuition. We note *std*, the standard deviation computed using all the numbers of representatives of the categories represented in a benchmark. The *std* of benchmarks generated using Algorithm 1 are null: their balance among category is preserved. We propose to get new benchmarks that have higher *std* by using the substitution operation. A substitution randomly removes a corruption c_1 from a benchmark *bench* and adds to it a corruption c_2 randomly selected in the set of candidates. But, c_1 and c_2 are selected such as three conditions are respected: (1) the represented categories of *bench* do not change (2) *std* of *bench* strictly increases (3) c_2 is not already in *bench*.

We consider *group*: a set of 1000 benchmarks that have been generated using Algorithm 1 with $n = 6, k = 2$. We get 5000 new benchmarks, by substituting from 1 to 5 corruptions of each benchmark in *group*. The obtained benchmarks have various *std*: (0.6, 0.8, 1.0, 1.2, 1.4, 1.5, 1.8, 2.2). We group together all the benchmarks with the same *std*. For each of these groups, we run Algorithm 2 for each of the following natural corruption benchmarks: ImageNet-A, ImageNet-R, ImageNet-V2 and ObjectNet. The group of neural networks used to run Algorithm 2 is the set of robust models presented in Table 1. The obtained results are displayed in Table 3. We observe that the computed scores decrease as the *std* of corruption benchmarks increase for all the considered natural corruption benchmarks. We repeat the experiment carried out in this section, using different benchmarks generated with Algorithm 2 with $n = 5, k = 3$ and $n = 6, k = 3$. For both n, k couples, the measured mean correlations also diminish as *std* of benchmarks increases. These experiments confirm that benchmarks for which balance among represented category is preserved, make robustness estimations more correlated with robustness to natural corruptions.

4.3 Corruption Benchmark Size

In Table 2, we observe that the scores obtained with the benchmarks generated using the n, k couples $(6, 1)$, $(6, 2)$ and $(6, 3)$; increase with k . We notice that rising k for a fixed n when using Algorithm 1, is equivalent to increase the size of generated benchmarks while conserving the balance among categories and the number of represented categories. Then, it appears that increasing the size of synthetic corruption benchmarks also helps to make robustness estimations more correlated with natural corruptions. To explain this, we see in Figure 2 that SCC are not completely correlated in terms of robustness. In other words, the representatives of the same category do not make exactly the same

	0.0	0.6	0.8	1.0	1.2	1.4	1.5	1.8	2.2
ImageNet-A	0.764	0.762	0.758	0.755	0.754	0.749	0.748	0.723	0.711
ImageNet-R	0.717	0.716	0.713	0.709	0.709	0.707	0.694	0.677	0.671
ImageNet-V2	0.806	0.808	0.808	0.799	0.780	0.772	0.773	0.725	0.670
ObjectNet	0.787	0.779	0.780	0.781	0.780	0.758	0.768	0.718	0.683

Table 3: Correlations computed with Algorithm 2 using natural corruption benchmarks (lines) and groups of synthetic corruption benchmarks that have various std values (columns).

	INet-A	INet-R	INet-V2	ObjectNet	Mean
ImageNet-C	0.62	0.51	0.89	0.80	0.71
ImageNet-Syn2Nat	0.77	0.71	0.85	0.81	0.79

Table 4: Robustness correlations of INet-Syn2Nat and INet-C to natural corruption benchmarks.

feature modifications. So, having more representatives in each category makes benchmarks measure the robustness to a larger range of feature modifications. Since natural corruptions modify a wide diversity of features in images, having more representatives per category (increasing k for a fixed n) should make robustness to corruption benchmarks more predictive of robustness to natural corruptions, which can explain the obtained results.

4.4 ImageNet-Syn2Nat

Starting from our 40 candidate corruptions, we use the three parameters identified in this section to constitute a benchmark that makes robustness estimations the most correlated as possible with robustness to natural corruptions. More precisely, the idea is to build the largest benchmark, that represents all the categories displayed in Figure 2 and has its balance among categories preserved. To respect these conditions, we consider all the categories, and we select the same number k of representatives per category, with the largest possible k . Three representatives are selected per category because the smallest category displayed in Figure 2 contains only three corruptions. For each category, we select the three corruptions that overlap the less with each other because we do not want to include corruptions that are almost equivalent. We group the selected corruptions to form a benchmark called ImageNet-Syn2Nat. The names of its 18 corruptions are underlined in Figure 2.

Now we want to estimate to what extent the robustness to ImageNet-Syn2Nat is predictive of robustness to natural corruptions. To achieve it, we compute the robustness of the fifteen models presented in Table 1 to ImageNet-Syn2Nat. Then, we compute the mean correlations between the robustness scores measured with ImageNet-Syn2Nat and the ones computed with other natural corruption benchmarks. The obtained scores are displayed in Table 4 and compared with the results obtained using another corruption benchmark (ImageNet-C [Hendrycks and Dietterich, 2019]). We observe that the robustness to ImageNet-Syn2Nat is much more correlated with the robustness to ImageNet-A and ImageNet-R than the robustness to ImageNet-C. For ImageNet-V2 and ObjectNet, the scores obtained with the two synthetic corruption benchmarks are relatively close. On average, we see that the robustness to ImageNet-Syn2Nat is more predictive of the robustness to the natural corruption benchmarks than the robustness to ImageNet-C.

5 Conclusion

We proposed a method to split a set of synthetic corruptions into some categories using the overlapping score. We showed that such categories are useful to better understand and address robustness of neural networks. Indeed, using corruption categories, we identified three parameters that are important to consider while building a corruption benchmark: the number of categories represented, the balance among categories and the size. We demonstrated that taking into account these parameters, helps to build corruption benchmarks that make robustness estimations more correlated with robustness to natural corruptions. We used these three parameters to build a new benchmark called ImageNet-Syn2Nat, that can be useful to complete existing ImageNet robustness benchmarks.

In further works, by using a larger set of candidate corruptions and by trying other clustering strategies, we would like to build more refined corruption categories than the ones presented in Figure 2. We also want to measure to what extent the robustness to ImageNet-Syn2Nat is predictive of the robustness to other natural corruption benchmarks such as ImageNet-D [Rusak et al., 2021]. We plan to adapt the methodology presented in this paper to other computer vision

tasks. We hope that these works will help to make robustness estimations that are more predictive of the observed robustness of neural networks in real world applications.

References

- Dan Hendrycks and Thomas Dietterich. Benchmarking neural network robustness to common corruptions and perturbations. *Proceedings of the International Conference on Learning Representations*, 2019.
- Christian Szegedy, Wojciech Zaremba, Ilya Sutskever, Joan Bruna, Dumitru Erhan, Ian Goodfellow, and Rob Fergus. Intriguing properties of neural networks. In *International Conference on Learning Representations*, 2014.
- Sara Beery, Grant Van Horn, and Pietro Perona. Recognition in terra incognita. In *Proceedings of the European Conference on Computer Vision (ECCV)*, September 2018.
- Evgenia Rusak, Lukas Schott, Roland S. Zimmermann, Julian Bitterwolf, Oliver Bringmann, Matthias Bethge, and Wieland Brendel. A simple way to make neural networks robust against diverse image corruptions. *ECCV*, 2020.
- Cihang Xie, Mingxing Tan, Boqing Gong, Jiang Wang, Alan L. Yuille, and Quoc V. Le. Adversarial examples improve image recognition. In *Proceedings of the IEEE/CVF Conference on Computer Vision and Pattern Recognition (CVPR)*, June 2020a.
- Qizhe Xie, Minh-Thang Luong, Eduard Hovy, and Quoc V. Le. Self-training with noisy student improves imagenet classification. In *Proceedings of the IEEE/CVF Conference on Computer Vision and Pattern Recognition (CVPR)*, June 2020b.
- Rohan Taori, Achal Dave, Vaishaal Shankar, Nicholas Carlini, Benjamin Recht, and Ludwig Schmidt. Measuring robustness to natural distribution shifts in image classification. In *NeurIPS*, 2020.
- Dan Hendrycks, Steven Basart, Norman Mu, Saurav Kadavath, Frank Wang, Evan Dorundo, Rahul Desai, Tyler Zhu, Samyak Parajuli, Mike Guo, Dawn Song, Jacob Steinhardt, and Justin Gilmer. The many faces of robustness: A critical analysis of out-of-distribution generalization. *arXiv preprint arXiv:2006.16241*, 2020.
- Alfred Laugros, Alice Caplier, and Matthieu Ospici. Using the overlapping score to improve corruption benchmarks. In *IEEE International Conference on Image Processing (ICIP)*, 2021.
- Josip Djolonga, Jessica Yung, Michael Tschannen, Rob Romijnders, Lucas Beyer, Alexander Kolesnikov, Joan Puigcerver, Matthias Minderer, Alexander Nicholas D’Amour, Dan Moldovan, Sylvain Gelly, Neil Houlsby, Xiaohua Zhai, and Mario Lucic. On robustness and transferability of convolutional neural networks. In *Conference on Computer Vision and Pattern Recognition*, 2021.
- Dan Hendrycks, Kevin Zhao, Steven Basart, Jacob Steinhardt, and Dawn Song. Natural adversarial examples. *CVPR*, 2021.
- Benjamin Recht, Rebecca Roelofs, Ludwig Schmidt, and Vaishaal Shankar. Do ImageNet classifiers generalize to ImageNet? In *Proceedings of the 36th International Conference on Machine Learning*, 2019.
- Logan Engstrom, Andrew Ilyas, Shibani Santurkar, Dimitris Tsipras, Jacob Steinhardt, and Aleksander Madry. Identifying statistical bias in dataset replication. In *Proceedings of the 37th International Conference on Machine Learning*, 2020.
- Andrei Barbu, David Mayo, Julian Alverio, William Luo, Christopher Wang, Dan Gutfreund, Josh Tenenbaum, and Boris Katz. Objectnet: A large-scale bias-controlled dataset for pushing the limits of object recognition models. In *Advances in Neural Information Processing Systems*, 2019.
- Vaishaal Shankar, Achal Dave, Rebecca Roelofs, Deva Ramanan, Benjamin Recht, and Ludwig Schmidt. A systematic framework for natural perturbations from videos. In *ICML Workshop on Identifying and Understanding Deep Learning Phenomena*, 2019.
- Evgenia. Rusak, Steffen Schneider, Peter Gehler, Oliver Bringmann, Wieland Brendel, and Matthias Bethge. Adapting imagenet-scale models to complex distribution shifts with self-learning. *CoRR*, abs/2104.12928, 2021.
- S. Karahan, M. Kilinc Yildirim, K. Kirtac, F. S. Rende, G. Butun, and H. K. Ekenel. How image degradations affect deep cnn-based face recognition? In *2016 International Conference of the Biometrics Special Interest Group (BIOSIG)*, pages 1–5, Sep. 2016.
- Claudio Michaelis, Benjamin Mitzkus, Robert Geirhos, Evgenia Rusak, Oliver Bringmann, Alexander Ecker, Matthias Bethge, and Wieland Brendel. Benchmarking robustness in object detection: Autonomous driving when winter is coming. *arXiv preprint arXiv:1907.07484*, 2019.
- Christoph Kamann and Carsten Rother. Benchmarking the robustness of semantic segmentation models. In *Proceedings of the IEEE/CVF Conference on Computer Vision and Pattern Recognition (CVPR)*, 2020.

- Zhaohui Che, Ali Borji, Guangtao Zhai, Xiongkuo Min, Guodong Guo, and Patrick Le Callet. How is gaze influenced by image transformations? dataset and model. *Trans. Img. Proc.*, 2020.
- Dogancan Temel, Gukyeong Kwon, Mohit Prabhushankar, and Ghassan AlRegib. Cure-tsr: Challenging unreal and real environments for traffic sign recognition. *NIPS Workshop*, 2017.
- Timothy Tadros, Nicholas C. Cullen, Michelle R. Greene, and Emily A. Cooper. Assessing neural network scene classification from degraded images. *ACM Trans. Appl. Percept.*, 2019.
- Dong Yin, Raphael Gontijo Lopes, Jonathon Shlens, Ekin D. Cubuk, and Justin Gilmer. A fourier perspective on model robustness in computer vision. *ICML Workshop on Uncertainty and Robustness in Deep Learning*, 2019.
- Alfred Laugros, Alice Caplier, and Matthieu Ospici. Are adversarial robustness and common perturbation robustness independent attributes? In *The IEEE International Conference on Computer Vision (ICCV) Workshops*, Oct 2019.
- J. Deng, W. Dong, R. Socher, L. Li, Kai Li, and Li Fei-Fei. Imagenet: A large-scale hierarchical image database. In *IEEE Conference on Computer Vision and Pattern Recognition*, 2009.
- Sungbin Lim, Ildoo Kim, Taesup Kim, Chiheon Kim, and Sungwoong Kim. Fast autoaugment. In *Advances in Neural Information Processing Systems*, 2019.
- Logan Engstrom, Brandon Tran, Dimitris Tsipras, Ludwig Schmidt, and Aleksander Madry. Exploring the landscape of spatial robustness. In Kamalika Chaudhuri and Ruslan Salakhutdinov, editors, *Proceedings of the 36th International Conference on Machine Learning*, volume 97 of *Proceedings of Machine Learning Research*, pages 1802–1811. PMLR, 2019.
- Robert Geirhos, Patricia Rubisch, Claudio Michaelis, Matthias Bethge, Felix A. Wichmann, and Wieland Brendel. Imagenet-trained CNNs are biased towards texture; increasing shape bias improves accuracy and robustness. In *International Conference on Learning Representations*, 2019.
- Dan Hendrycks*, Norman Mu*, Ekin Dogus Cubuk, Barret Zoph, Justin Gilmer, and Balaji Lakshminarayanan. Augmix: A simple method to improve robustness and uncertainty under data shift. In *International Conference on Learning Representations*, 2020.
- Junnan Li, Caiming Xiong, and Steven Hoi. Mopro: Webly supervised learning with momentum prototypes. In *International Conference on Learning Representations*, 2021.
- Zeyi Huang, Haohan Wang, Eric P. Xing, and Dong Huang. Self-challenging improves cross-domain generalization. In *ECCV*, 2020.
- Aleksander Madry, Aleksandar Makelov, Ludwig Schmidt, Dimitris Tsipras, and Adrian Vladu. Towards deep learning models resistant to adversarial attacks. In *International Conference on Learning Representations*, 2018.
- Cristina Vasconcelos, Hugo Larochelle, Vincent Dumoulin, Nicolas Le Roux, and Ross Goroshin. An effective anti-aliasing approach for residual networks. *ArXiv, abs/2011.10675*, 2020.
- Sangdoon Yun, Dongyoon Han, Seong Joon Oh, Sanghyuk Chun, Junsuk Choe, and Youngjoon Yoo. Cutmix: Regularization strategy to train strong classifiers with localizable features. In *Proceedings of the IEEE/CVF International Conference on Computer Vision (ICCV)*, October 2019.
- Dhruv Kumar Mahajan, Ross B. Girshick, Vignesh Ramanathan, Kaiming He, Manohar Paluri, Yixuan Li, Ashwin Bharambe, and Laurens van der Maaten. Exploring the limits of weakly supervised pretraining. In *ECCV*, 2018.
- I. Zeki Yalniz, Hervé Jégou, Kan Chen, Manohar Paluri, and Dhruv Mahajan. Billion-scale semi-supervised learning for image classification. *arXiv preprint arXiv:1905.00546*, 2019.
- Alexander Buslaev, Vladimir I. Iglovikov, Eugene Khvedchenya, Alex Parinov, Mikhail Druzhinin, and Alexandr A. Kalinin. Alumentations: Fast and flexible image augmentations. *Information*, 2020. ISSN 2078-2489. doi:10.3390/info11020125.